https://doi.org/10.37434/tpwj2020.01.01

PROCESSES OF NONCONSUMABLE ELECTRODE WELDING WITH WELDING CURRENT MODULATION (Review) Part III. Modeling of the processes of TIG welding by modulated current

Boyi Wu[1] and **I.V. Krivtsun**[2]

[1]Guangdong Institute of Welding (China-Ukraine E.O. Paton Institute of Welding)
363 Chiansin Str., 510650, Guangzhou, Tianhe. E-mail: wuby@gwi.gd.cn
[2]E.O. Paton Electric Welding Institute of the NAS of Ukraine
11 Kazymyr Malevych Str., 03150, Kyiv, Ukraine. E-mail: office@paton.kiev.ua

A review of investigations devoted to the processes of inert-gas nonconsumable electrode welding with welding current modulation was performed. The third part of the review is devoted to analysis of the works, dealing with theoretical study and mathematical modeling of the processes of heat-, mass- and electric transfer in arc plasma and welded metal in TIG welding by modulated current. Different approaches to theoretical study of the above-mentioned processes are described, as well as respective mathematical models, allowing for the conditions of nonconsumable electrode welding with low-frequency (up to 10 Hz) and high-frequency (above 10 kHz) pulse modulation of welding current. Results of numerical analysis of the distributed and integral characteristics of an argon arc with refractory cathode at pulse variation of current are given. It was performed on the base of models of a nonstationary arc with distributed and concentrated parameters. Results of computer modeling of thermal, hydrodynamic and electromagnetic processes in the welded metal (also at self-consistent accounting of the processes that proceed in arc plasma) were analyzed for the case of spot TIG welding with low-frequency pulse modulation of current. Presented are the analytical dependencies that describe the impact of the shape and parameters of welding current pulses on the characteristics of dynamic action of an arc with a refractory cathode on weld pool metal. 21 Ref., 4 Tables, 19 Figures.

Keywords: arc with refractory cathode, TIG welding, arc plasma, metal being welded, penetration, welding current modulation, pulse, frequency, duty cycle, amplitude, mathematical modeling

The features of arc burning, metal penetration and weld formation in nonconsumable electrode welding with welding current modulation, considered in the first [1] and second [2] parts of this review, which were established experimentally, required conducting theoretical investigations, development of mathematical models and numerical modeling of the above-mentioned processes, in order to clarify and predict the nature of their passage at practical realization of different technologies of TIG welding by modulated current.

In work [3] it is assumed that the effect of the arc contraction at HFP modulation of current, which is observed experimentally, and increase of its pressure on weld pool surface, compared with an arc of direct current, equal to average value of modulated current, is related to increase of effective value of modulated current, compared to its average value. This assumption is written as the following ratio

$$P_{PC} = P_{DC} \frac{I_{eff}^2}{I_{av}^2}, \quad (1)$$

where P_{PC} is the pressure of modulated current arc; P_{DC} is the pressure of direct current arc; I_{eff}, I_{av} is the effective and average value of current.

By the data of work [3], the thus calculated arc pressure at HFP modulation of current fits in well with experimental data.

At modulation of arc current by rectangular and triangular pulses the square of effective value of current can be approximately calculated as follows:

$$I_{eff}^2 \approx I_p I_{av} \quad (2)$$

for rectangular pulses and

$$I_{eff}^2 \approx \frac{2}{3} I_p I_{av} \quad (3)$$

for triangular pulses, where I_p is the peak value of current (when writing (2), (3), it was assumed that base current value I_b is much smaller than I_p).

As in the frequency range f = 10–20 kHz the pulse shape is close to a triangular one, peak current at fixed power of the power source (by direct current) can be assessed by the following ratio:

$$I_p \sqrt{\frac{I_{av}}{fL}}, \quad (4)$$

I.V. Krivtsun — http://orcid.org/0000-0001-9818-3383

where L is the welding circuit inductance.

In this case, using (1), (3), (4), the ratio of pressure of an arc with HFP modulation of current to that of an arc of direct current (that characterizes the degree of arc constriction) can be presented in the following form

$$\frac{P_{PC}}{P_{DC}} \sim \sqrt{\frac{1}{I_{av} fL}}. \quad (5)$$

Thus, the effect of arc constriction at HFP modulation of current is the most pronounced in the cases of small values of average current.

Work [4] is devoted to comparative analysis of pressure on weld pool surface that is applied by an arc with nonconsumable electrode at pulse modulation of welding current and by an arc of direct current, the value of which is determined under the condition of equal power of the considered arcs. At evaluation of arc pressure the authors used the assumption that the current channel has the shape of a truncated cone with the height equal to arc length that expands from the cathode, where the channel radius is selected equal to r_0 towards the anode where the radius is equal to R ($R > r_0$). It is assumed that the current density is uniformly distributed over the cross-section of the current channel. This allows writing the pressure of an arc of constant current I_c on the anode surface in the following form

$$P_C = \frac{\mu I_c^2}{4\pi^2 R^2} \ln\left(\frac{R}{r_0}\right), \quad (6)$$

where μ is the universal magnetic constant.

The power of constant current arc is defined as the product of current I_c by voltage $U(I_c)$ that is calculated using the approximation of the measured experimental static volt-ampere characteristics (VAC) of the arc:

$$U(I) = B_1 I + B_2 + B_3/I, \quad (7)$$

where B_1, B_2, B_3 are the constant coefficients, which depend on arc burning conditions.

In view of [7], the power of an arc of constant current I_c can be written as follows:

$$W_C = B_1 I_c^2 + B_2 I_c + B_3. \quad (8)$$

In the case of an arc of modulated current, assuming that modulation is performed by rectangular pulses with duty cycle δ, the average and effective value of current can be calculated by the following expressions:

$$I_{av} = \delta I_p + (1-\delta) I_b; \; I_{eff} = \left[\delta I_p^2 + (1-\delta) I_b^2\right]^{1/2}, \quad (9)$$

where I_p, I_b are the peak and base current values.

Average value of power of such an arc $W_P \equiv \frac{1}{T}\int_0^T I(t)U(t)dt$ in work [4] is defined under the condition that the change of arc voltage in time at the change of current takes place along a static VAC (7) that gives

$$W_P = B_1 I_{eff}^2 + B_2 I_{av} + B_3. \quad (10)$$

It should be noted that the last assumption essentially limits the modulation frequency, with increase of which the change of voltage at the change of arc current that occurs in keeping with a dynamic VAC of the arc, differs ever more from dependence (7) [5].

Comparing expressions (8) and (10), the authors find duty cycle δ which at set I_c, I_p, I_b values provides the condition of equality of powers of the arc for constant and modulated current:

$$\delta = \frac{B_1\left(I_c^2 - I_b^2\right) + B_2\left(I_c - I_b\right)}{B_1\left(I_p^2 - I_b^2\right) + B_2\left(I_p - I_b\right)}. \quad (11)$$

Assuming further that the dimensions of the current channel of an arc with pulse modulation of current are equal to respective dimensions for an arc of constant current and using expression (6), the authors of [4] write

$$P_P = \frac{\mu I_{eff}^2}{4\pi^2 R^2} \ln\left(\frac{R}{r_0}\right), \quad (12)$$

that leads them to a conclusion, similar to the one made in work [3] (see (1)), namely:

$$P_R \equiv P_P / P_C = I_{eff}^2 / I_c^2. \quad (13)$$

Using the obtained relationships, work [4] gives the calculated dependencies of P_R, W_p, I_{eff}/I_{av}, as well as I_c, I_{av}, I_{eff} on the duty cycle at the following parameters of arc burning mode: arc length of 1 mm, shielding gas Ar, I_p = 500 A, I_b = 5 A. For instance Figure 1 gives dependence $P_R(\delta)$ which shows that pressure on the surface of the anode of an arc with pulse modulation of current at small values of the duty cycle can be ten and more times higher than the relative value of an arc of constant current (δ = 1).

In work [6] a computer modeling of thermal, hydrodynamic and electromagnetic processes in metal being welded was performed at spot argon-arc welding (welding by a stationary arc) of a sample from 3 mm stainless steel AISI 304 by an arc burning at constant current and with low-frequency modulation of welding current by rectangular pulses. The follow-

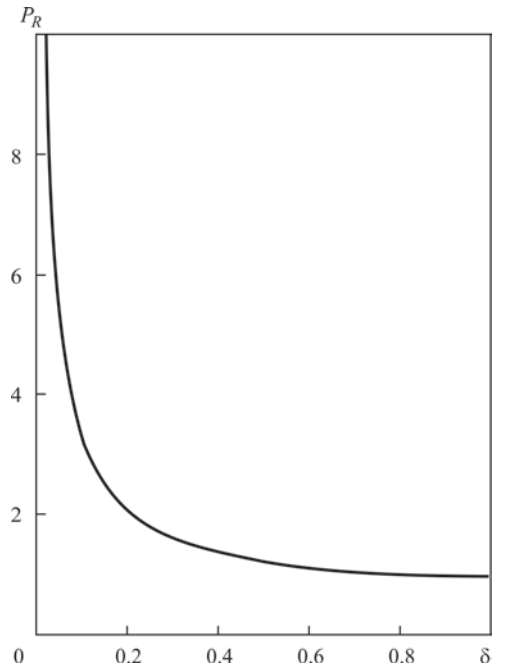

Figure 1. Dependence of the ratio of pressure on the anode surface of modulated current arc to pressure of a direct current arc on the duty cycle at the same power (I_b = 5 A, I_p = 500 A, 1 mm arc length) [4]

ing assumptions were used when constructing the mathematical model: 1) considered system is assumed to be axisymmetric; 2) molten metal is a viscous liquid which is incompressible, its flow in the weld pool is laminar; 3) at analysis of hydrodynamic processes in the metal pool the Lorenz and Archimedean forces acting in the pool volume were taken into account, as well as Marangoni force, pressure and force of friction

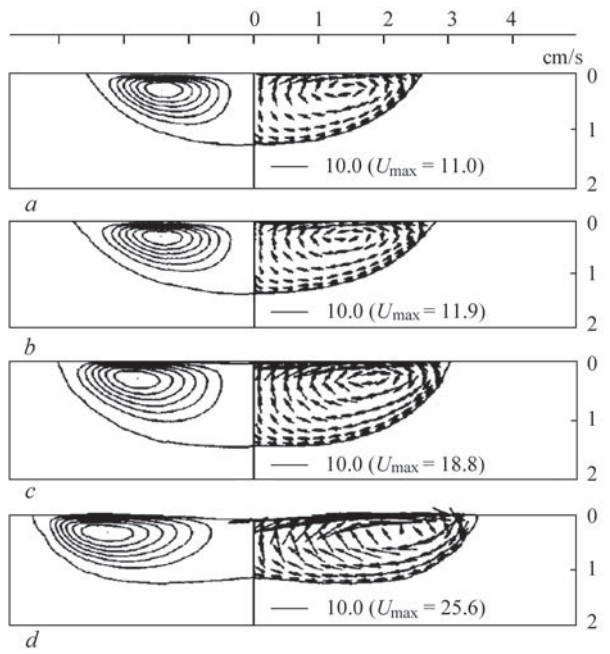

Figure 2. Patterns of the flow (left) and fields of movement velocities (right) of the melt at the action on welded metal for 1.92 s: *a* — direct current arc (100 A); *b*–*d* — modulated current arc (variants 1–3 in Table 1, respectively) [6]

Table 1. Parameters of burning mode of an arc with current modulation [6]

Parameter	Variant 1	Variant 2	Variant 3
Base current I_b, A	36	40	48
Pause duration t_b, s	0.16	0.24	0.32
Peak current I_p, A	120	136	160
Pulse duration t_p, s	0.32	0.24	0.16
Effective current I_E, A	100	100	100
Mean current I_M, A	92	88	85
Duty cycle r_I	0.67	0.50	0.33
Frequency F_i, Hz	2.08	2.08	2.08
Ratio t_p/t_b	2.0	1.0	0.5
Ratio I_M/I_E	0.92	0.88	0.85

of arc plasma on the pool surface; 4) welded metal properties are assumed independent on temperature, except for the surface tension factor, density, specific heat capacity and heat conductivity factor; 5) distribution of the heat flow, electric current density, pressure and force of friction of arc plasma on the surface of the metal being welded were determined on the base of the results of modeling a constant current arc [7, 8] at different current values (quasistationary arc).

Numerical modeling was performed using the parameters of the mode of burning of an arc of modulated current (Table 1) and constant current given below.

Параметри режиму горіння дуги постійного струму [6]

Arc length, mm 2.0
Arc current, A 100
Arc voltage, V 14.0
Electrode ..... W + 2 % Th
Electrode diameter, mm 3.2
Electrode sharpening angle, deg 60
Nozzle diameter, mm 12.7
Shielding gas flow rate (Ar), l/min 10.0

Figure 2 shows patterns of the flow and fields of velocities (cm/s) of weld pool liquid metal (arc of direct and modulated current) for 1.92 s.

Results of conducted in work [6] computer modeling allowed the authors to conclude that increase of t_p/t_b ratio or duty cycle results in increase of penetration depth at other conditions being equal.

Work [9] is also devoted to modeling the processes proceeding in the metal being welded at TIG welding with low-frequency modulation of arc current. Thermal, hydrodynamic and electromagnetic processes in a 3 mm sample of stainless steel 304 were considered at the following parameters of the welding mode: arc voltage U = 13 V, welding current is modulated by rectangular pulses, durations of the pulse t_p and pause t_b were assigned as t_p = t_b = 1 s, pulse current I_p = = 170 A, base current I_b = 35 A, welding speed v = = 1.6 mm/s. The mathematical model was constructed

using the following assumptions: 1) weld pool metal is assumed to be a viscous incompressible liquid, flowing mode is laminar; 2) distributions of the heat flow, current density and arc pressure on the sample surface are Gaussian; 3) properties of the metal being welded are independent on temperature, expect for the melt surface tension factor (in order to allow for Marangoni effect); 4) weld pool surface is considered to be flat.

Figure 3 shows the calculated dependencies of penetration depth and weld half-width on welding time. As follows from the presented curves, the most marked changes of weld depth and width with the change of arc current are observed at the very start of the welding process (t < 4 s). After four periods of welding current alternation the amplitude of oscillation of the considered characteristics somewhat decreases, their maximum and minimum values becoming practically independent on time.

In order to verify the developed model, the authors of [9] performed comparison of calculated data with experimental ones, obtained by video recording of weld pool surface. As it was impossible to conduct such video recording during the action of current pulse I_p, Figure 4 gives the data on the change of weld width only during arc burning at minimum current I_b. Comparison of calculated and experimental data showed their quite satisfactory agreement.

Book [10] is devoted to detailed description of the currently available approaches and mathematical models used for modeling the thermal and hydrodynamic processes in the metal being welded at different methods of arc (MIG/MAG, TIG) and plasma welding. The equations of the respective mathematical models are written in a nonstationary form that allows using them for modeling the processes of arc welding both by constant current and with pulse modulation of arc current.

In works [11, 12] a detailed numerical study was performed of the processes of spot TIG welding (welding by a stationary heat source) of stainless steel AISI 304 at low-frequency modulation of welding current by rectangular pulses in the form of a meander. Work [11] proposes a 2D model of thermal, hydrodynamic and electromagnetic processes in the metal being welded at its partial (10 mm thick sample) and complete (4 mm thick sample) penetration. When constructing the model, the authors used the following assumptions: 1) considered system has axial symmetry; 2) molten metal is a viscous incompressible liquid, flow mode is laminar; 3) metal flow in the weld pool forms due to action of Archimedean, Lorenz and Marangoni forces (force of friction of plasma flow against the melt surface is ignored), as

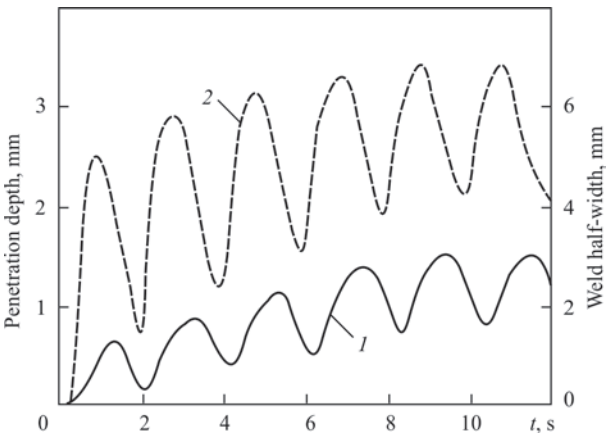

Figure 3. Dependencies of penetration depth (*1*) and weld half-width (*2*) on time [9]

well as pressure of arc plasma on the pool surface; 4) the energy equation takes into account the latent heat of melting-solidification; 5) characteristics of the electromagnetic field in the metal being welded are defined taking into account the eddy currents. Distributions of electric current density, heat flow and arc pressure on the welded metal surface required for determination of boundary conditions on this surface, were assigned based on the respective distributions for direct current arcs in the range of 80–200 A. However, the authors of [11] did not specify the reference from which these data were taken. Calculations were conducted using the parameters of pulse modulation of welding current given below. Weld pool behaviour was considered for 3.5 s from the start of the welding process (7, 14 and 21 modulation period at 2, 4, and 6 Hz frequency, respectively).

Parameters of arc current modulation [11]

Maximum peak value of current I_p, A	200
Minimum base value of current I_b, A	80
Pulse duration t_p, s	0.25; 0.125; 0.083
Pause duration t_b, s	0.25; 0.125; 0.083
Frequency f, Hz	2; 4; 6

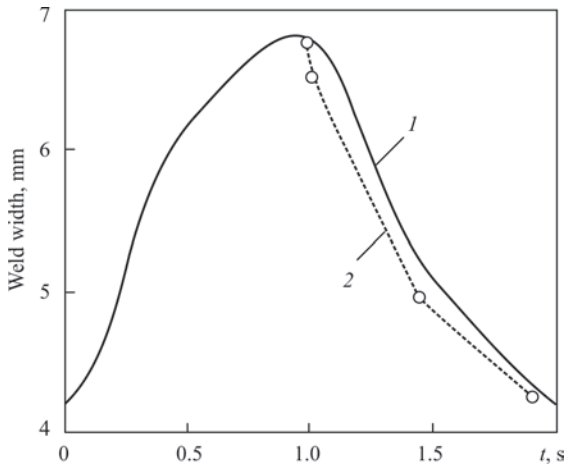

Figure 4. Comparison of calculated (*1*) and experimental (*2*) dependence of weld width on time for one period of welding current modulation [9]

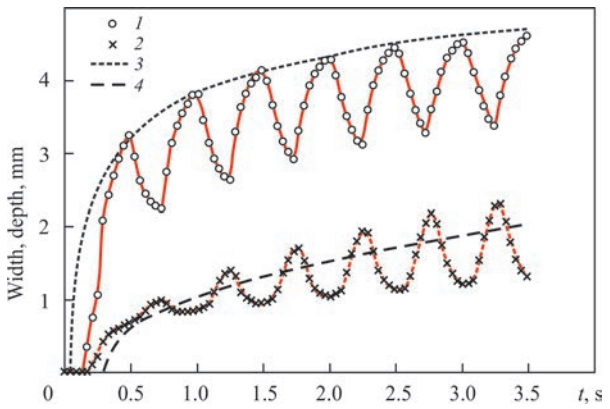

Figure 5. Time dependencies of penetration width (*1*) and depth (*2*) in TIG welding by modulated current, compared to penetration width (*3*) and depth (*4*) in direct current welding [11]

Figure 5 presents calculated dependencies of penetration width (weld spot diameter) and depth during welding 10 mm sample at pulse modulation of arc current in the range of 80–200 A (140 A average current) that is performed at 2 Hz frequency, compared to the respective dependencies at spot welding by constant current of 170 A.

The calculated data given in this Figure show that the change in time of weld pool maximum diameter at pulse modulation of arc current corresponds to the behaviour of pool diameter in welding at constant current of 170 A. At the same time, the energy applied to the sample during 3.5 s is equal to 4565 J in the first case, whereas in the second case this energy turns out to be much greater and equal to 5867 J, that is an important advantage of TIG welding with pulse modulation of current, as it allows lowering the residual stresses and strains.

Another important feature of TIG welding by modulated current is a considerable change of weld pool surface shape in time. Characteristic shapes of the pool surface during the pulse and pause of current for the above modulation mode are shown in Figure 6.

Figure 7 gives the calculated data on time dependence of weld pool dimensions at complete penetration of 4 mm sample in the case of spot welding

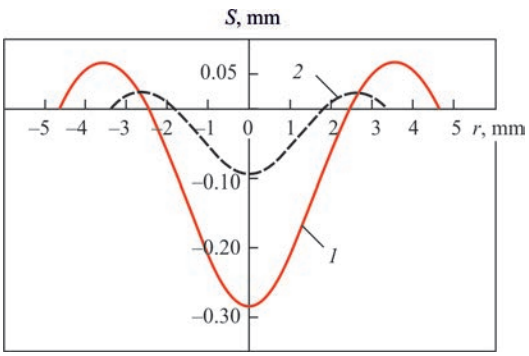

Figure 6. Shapes of weld pool surface at peak (*1* — 200 A) and base (*2* — 80 A) values of arc current after six periods of modulation at 2 Hz frequency [11]

with pulse modulation of arc current in the range of 80–200 A at 2 Hz frequency.

In order to verify the proposed model, the calculated geometrical dimensions and shape of penetration of a 10 mm sample at the action of a modulated current arc on it for 3.5 s were compared with the respective dimensions and shape of macrosections of weld spots, determined experimentally. The results of such a comparison are given in Figure 8 for different values of current modulation amplitude (average value of current of 140 A) at the frequency of 2 Hz. These results are indicative of sufficient adequacy of the mathematical model, proposed by the authors [11].

In work [12] the considered model was generalized for self-consistent accounting for the processes that proceed in the electrode (cathode), arc column and metal being welded at spot TIG welding with a low-frequency modulation of current. Such a generalized model was used to perform a detailed computer modeling of the above-listed processes in welding samples of the same steel (AISI 304) 8 and 4 mm thick by a 3 mm argon arc with tungsten cathode of 3.2 mm diameter (sharpening angle of 60 deg) at the following parameters of current modulation: rectangular pulses in the form of a meander, repetition rate of 1 Hz; pulse current I_p = 160 A, pause current I_b = 80 A.

Figure 9, *a* gives the results of comparison of the dynamics of the change in time of weld pool half-width calculated on the base of model [12], and determined experimentally by video recording of weld pool surface, at spot TIG welding of an 8 mm sample by an argon arc of modulated current with the above-given parameters. Figure 9, *b* shows the calculated shape and dimensions of penetration zone of the metal being welded, as well as the respective macrosection of the weld spot, achieved during 15 s of the arc action on the sample being welded. As follows from com-

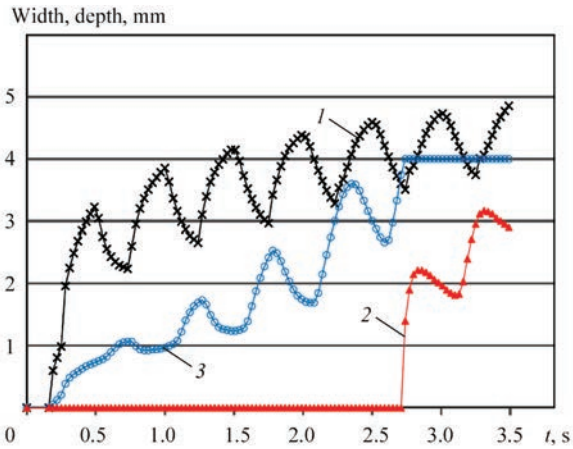

Figure 7. Time dependencies of weld pool width from the face (*1*) and reverse (*2*) sides of the sample, as well as penetration depth (*3*) at spot TIG welding by modulated current with complete penetration [11]

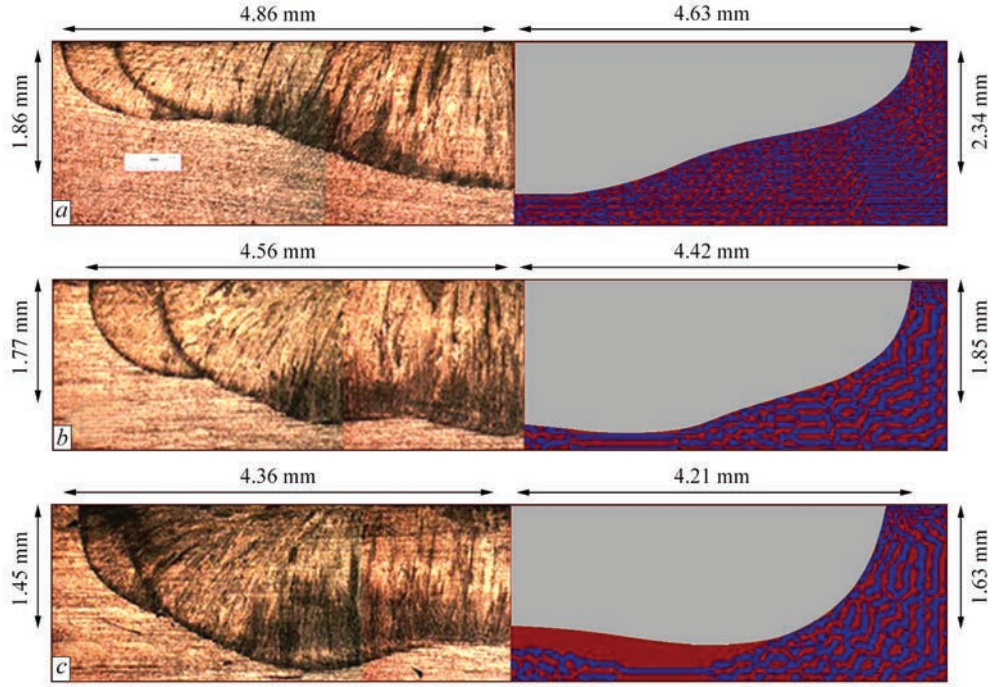

Figure 8. Macrosections of weld spots (left) and calculated shapes of metal penetration (right) at spot TIG welding of samples from steel AISI 304 with low-frequency modulation of current in the following range: *a* — 80–200; *b* — 100–180; *c* — 120–160 A [11]

parison of modeling results and experimental data, the proposed by the authors [12] mathematical model allows predicting with a high accuracy, both the dynamics of the change of geometrical characteristics of the weld pool, and the resultant shape of the penetration zone, achieved in a certain time.

Work [13] of the Chinese scientists is devoted to studying the electromagnetic force that acts on the arc plasma at TIG welding with high-frequency (f = = 20–80 kHz) pulse modulation of welding current.

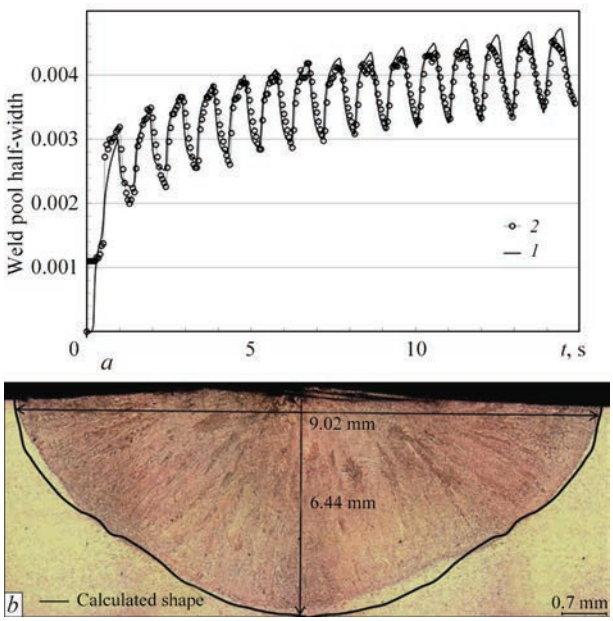

Figure 9. Comparison of calculated (*1*) and experimental (*2*) data by the dynamics of the change of weld pool half-width (*a*) and resultant form of penetration zone (*b*) in spot TIG welding by modulated current [12]

The authors assume that the current density in the arc column has, as shown in Figure 10 an axial and radial components, and is distributed by Gaussian law:

$$\begin{cases} J_z = \dfrac{Id}{\pi R_r^2} \exp\left(-\dfrac{r^2 d}{R_r^2}\right); \\ J_r = J_z \, \mathrm{tg}\varphi, \end{cases} \qquad (14)$$

where I is the arc current; d = 3 is the concentration coefficient; R_r is the radius of electrically conducting section of the arc column, which is considered to be conical; φ is the angle of inclination of the current line to the arc axis (see Figure 10). This allows writing the expressions for the components of electromagnetic force acting on the plasma, in the following form:

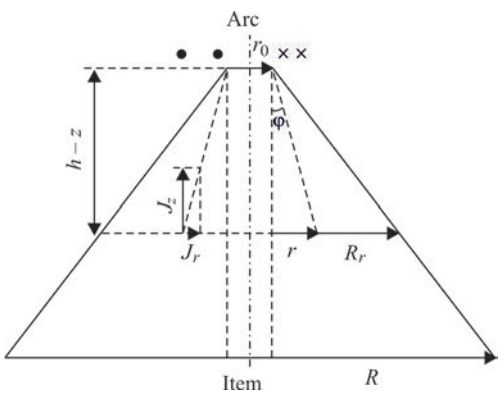

Figure 10. Scheme of distribution of current density in the arc column [13]

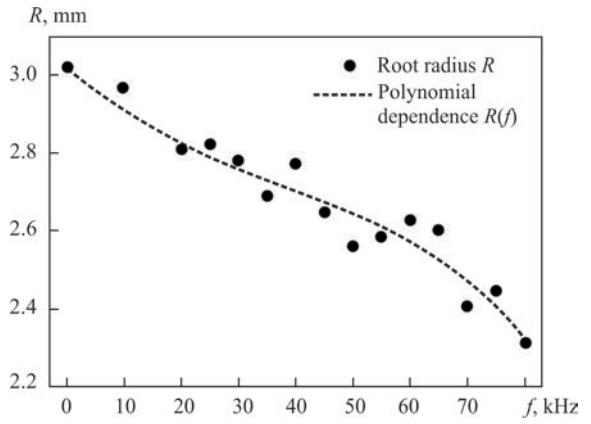

Figure 11. Arc root radius, depending on current modulation frequency [13]

$$\begin{cases} F_r = C_1 t \exp(-t)\left[1-\exp(-t)\right]; \\ F_z = 0, (r \le r_0); C_2 t \exp(-t)\left[1-\exp(-t)\right], \\ (r \ge r_0). \end{cases} \quad (15)$$

Here $t = r^2 d / R_r^2$; $C_1 = -\mu I^2/(2\pi^2 r^2 (h-z)$; $C_2 = -\mu I^2 (r - r_0)/[2\pi^2 r^2 (h-z)]$; where μ is the magnetic permeability; h is the arc length; coordinate z is calculated from the item surface. It should be noted that the expression for F_z (formulas (4) and (6)) in work [13] is written incorrectly.

Alongside the distributed characteristics of electromagnetic force in the arc column, such an integral characteristic of force action as arc pressure on anode surface, which written in the following form, was also studied in this work (see also [4]):

$$P_{ez} = \frac{\mu I^2}{4\pi^2 R^2} \ln \frac{R}{r_0}. \quad (16)$$

At analysis of this dependence, it is assumed that value r_0 is constant and is equal to half of electrode diameter. Arc root radius R is determined experimentally by photo recording of the transverse size of the arc anode zone in TIG welding of titanium alloy Ti–6Al–4V 2.5 mm thick with different frequencies of welding current modulation. Experiments were performed using 3 mm argon arc with refractory (W + + 2 % Ce) cathode of 2.4 mm diameter; welding mode parameters are given in Table 2.

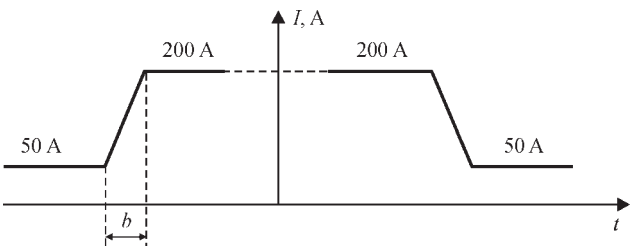

Figure 12. Diagram of pulsed change of arc current [14]

Table 2. Parameters of the studied welding modes [13]

Experiment number	Base current I_b, A	Pulse current I_p, A	Frequency f, kHz	Duty cycle δ, %
1	75	–	–	–
2–14	40	100	20–80	50

Figure 11 shows the dependence of arc root radius on current modulation frequency, which is indicative of increase of the degree of arc contraction on the anode (reduction of R) with frequency increase. The following polynomial dependence was proposed for approximation of the derived experimental data: $R(f) = -0.0014f^3 + 0.0307f^2 - 0.2755f + 6.2086$.

Rewriting formula (16) in the following form $P_{ez} = \frac{\mu I^2}{4\pi^2 r_0^2} \frac{1}{n^2} \ln n$, where $n = \frac{R}{r_0}$, and studying this expression, the authors of [13] find that at $n < 1.6$ (more exactly, at $n < \exp(1/2)$) value P_{ez} is an ascending function of n, and at $n > 1.6$ it is a descending function. It means that the arc pressure on the anode surface becomes greater with increase of R at $R < R_c$ and decreases at $R > R_c$, where for the set value r_0 = = 1.2 mm the critical value of arc root radius R_c is equal to 1.92 mm.

As, according to experimental data, given in Figure 11, value R turns out to be greater than R_c for all the values of modulation frequency and decreases with f increase, the conclusion is made that with increase of current modulation frequency the pressure of the arc on the weld pool surface rises, that leads to the heat source moving deeper into the metal being welded, and, therefore, to increase of the arc penetrability.

In work [14], the self-consistent mathematical model of nonstationary processes of energy-. mass- and electric transfer in the column and anode region of the electric arc with a refractory cathode [15] was the base to perform a detailed numerical analysis of the characteristics of an argon arc with a copper water-cooled anode at pulsed change of electric current (Figure 12).

It is found that arc burning at an abrupt increase (decrease) of current is accompanied by an essential restructuring of the electromagnetic, thermal and gas-dynamic characteristics of arc plasma, as well as the characteristics of its action on the anode surface. Here, the dynamic behaviour of the above-mentioned characteristics depends not only on the rate of arc current change, but also on its increasing or decreasing. Here, at a high rate of current change $\left(\left|\frac{dI}{dt}\right| > 5 \cdot 10^6 \text{ A/s}\right)$ the change of the arc column and anode region characteristics proceeds in two stages,

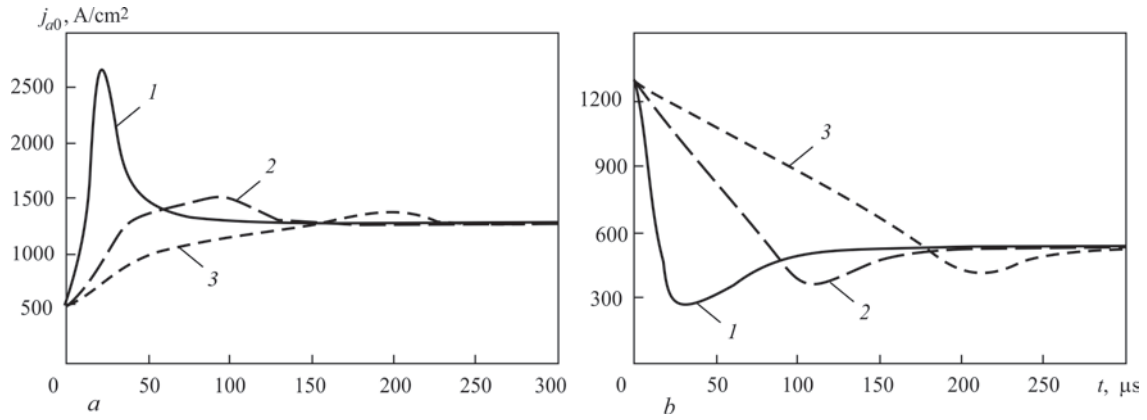

Figure 13. Change of axial value of electric current density on the anode at pulsed increase (*a*) and decrease (*b*) of arc current (*1* — *b* = = 20; *2* — 100; *3* — 200 μs) [14]

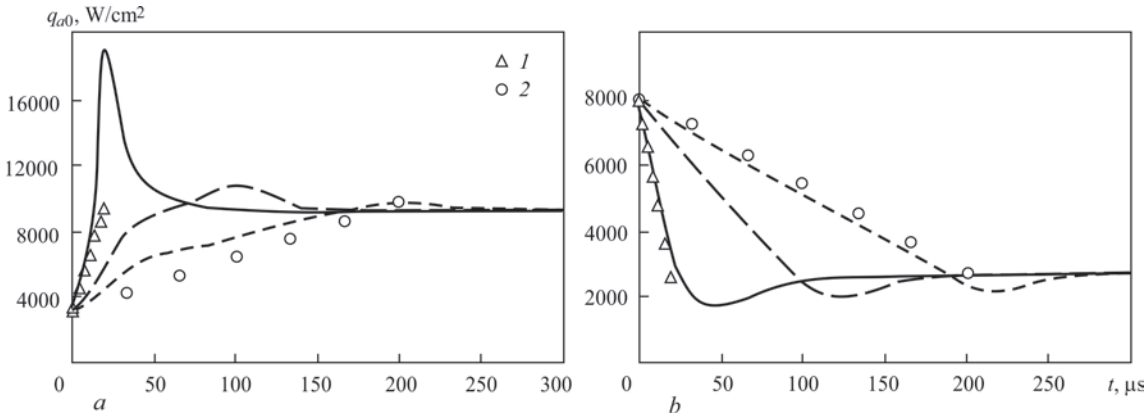

Figure 14. Change of axial value of the density of heat flow to the anode at pulsed increase (*a*) and decrease (*b*) of arc current (markers show values q_{a0} for a stationary arc at respective current values: *1* — *b* = 20; *2* — 200 μm) [14]

namely stage of the change together with arc current and stage of transient processes. As follows from the calculated data given in Figures 13, 14, at increase (decrease) of arc current the density of electric current and heat flow on the anode can become two times higher (1.5 times smaller) then the respective values for an arc of direct current equal to the larger (smaller) value, respectively.

At the transient process stage, relaxation of the thermal and gas-dynamic state of arc plasma to values characteristic for a stationary arc at the respective current value, takes place. Durations of the relaxation processes depend on values of maximum and minimum current, and can differ essentially from the local and integral characteristics of arc column plasma and anode region.

At current change at a rate lower than 10^6 A (b > > 100 μs), the processes associated with increase (decrease) of current and relaxation processes proceed simultaneously. As a result of that the nonstationary process of arc burning is realized in the form of a successive change of states, characteristic for a stationary arc at the respective current values (see, for instance, Figure 14), that is the change of arc characteristics occurs in the quasistationary mode.

Work [16] is devoted to investigation of the impact of high-frequency pulse modulation of current on depression of weld pool surface in TIG welding of samples of 2.5 mm titanium alloy Ti–6Al–4V. This study includes experimental measurement of the force, with which the arc acts on the surface of the sample being welded, and geometrical characteristics of its penetration (weld width *B* and penetration depth *H*), as well as mathematical modeling of the processes proceeding in the metal being welded, taking into account the depression of the free surface of the weld pool.

A special test rig, which allows measuring the force acting on the sample in TIG welding, was developed, in order to conduct the experiments. A 3 mm argon arc with refractory (W + 2 % Ce) cathode of 1.2 mm radius was used in the experiments, welding mode parameters are given in Table 3, welding speed

Table 3. Welding mode parameters [16]

Experiment number	Base current I_b, A	Pulse current I_p, A	Frequency f, kHz	Duty cycle δ, %
1	80	–	–	–
2	40	100	20	50
3	40	100	40	50
4	40	100	60	50
5	40	100	80	50

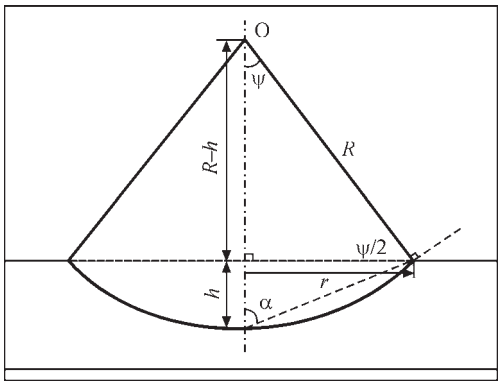

Figure 15. Approximation of weld pool free surface [16]

was constant and equal to 150 mm/min in all the experiments.

For mathematical modeling of thermal, hydrodynamic and electromagnetic processes in the metal being welded, a 2D model was used, which was constructed with the following assumptions: 1) molten metal is a viscous incompressible liquid, its flow in the weld pool is laminar; 2) at analysis of hydrodynamic processes in the weld pool the volumetric forces (Lorenz and Archimedean), as well as surface forces (Marangoni and arc pressure) are taken into account; 3) properties of the material being welded are considered to be independent on temperature, except for specific heat capacity and heat conductivity factor, as well as surface tension factor, viscosity and density of the melt (Boissinesq approximation).

At evaluation of the degree of curving of the weld pool free surface, its approximation by part of a spherical surface was used, as shown in Figure 15.

Writing the balance of forces on this surface, the authors of [16] obtain the following expression:

$$\Phi(h) = F - \frac{\pi}{6}\rho g h^3 - \frac{3\pi}{2}\rho g r^2 h - 8\sigma r \operatorname{arctg}\frac{h}{r}, \quad (17)$$

where F is the force of arc action on the surface of metal being welded; ρ, σ is the density and surface tension factor of the melt; g is the free fall acceleration; r, h are the weld pool radius and depression of its free surface (see Figure 15). The root of equation $\Phi(h) = 0$ corresponds to value h, at which the balance of forces is fulfilled (17).

Weld pool radius r, included into equation (17), was defined as half of experimentally measured value of weld width B. After that dependencies $\Phi(h)$ were plotted for different values of modulation frequency, which are presented in Figure 16. The same Figure shows the respective values of the roots of equation $\Phi(h) = 0$.

The experimental and calculated values of parameters which determine the depression of weld pool surface are given in Table 4.

Completing the review of work [16], it should be noted that force F, which is measured experimentally, contains two components — the force proper of action of arc plasma on the metal being welded and force acting on the sample being welded, due to current flowing in its volume (a similar force, acting on arc column plasma, was defined in [4]). Calculations show that, for instance, at arc current, equal to 178 A, the force acting on a sample from 5 mm stainless steel, is equal to 4.4 mN. Thus, the used in [16] values of the force of arc action on weld pool surface, and, hence, of depression of this surface, are much too high.

In work [17] an attempt was made to analyze the force of action of arc plasma flow on the surface of the metal being welded at TIG welding with HFP modulation of arc current. Without any substantiation, the authors assume that the distribution of plasma flow pressure in the area of anode binding of the arc has the following form:

$$P_r = P_{peak} \exp\left(-a|r|\right), \quad (18)$$

where P_{peak} is the gas-dynamic pressure on the arc axis; a is the distribution coefficient; r is the radial coordinate. Then the value of the respective force acting on weld pool surface is mathematically incorrectly calculated, and it is compared with experimentally measured (by the procedure described in [16]) value of this force, which, as was noted above, is greatly

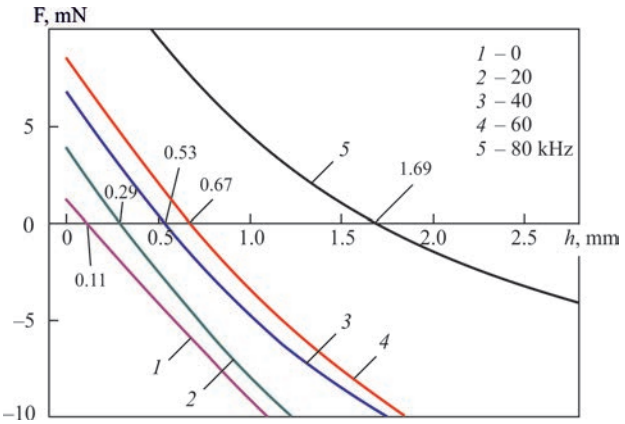

Figure 16. F(h) dependencies at different values of arc current modulation frequency [16]

Table 4. Values of parameters that determine the weld pool surface depression [16]

Frequency f, Hz	Force action of the arc F, mN	Weld width B, mm	Penetration depth H, mm	Surface depression h, mm
0	1.79	4.16	2.29	0.11
20	4.19	3.10	1.75	0.29
40	7.00	2.77	1.85	0.53
60	8.84	3.21	2.15	0.67
80	16.06	2.59	2.06	1.63

overestimated. Therefore, the conclusions made in work [17] do not seem to be reasonable.

Work [5] is devoted to use of the model of a non-stationary arc with concentrated parameters for analysis of the dynamics of the change of its characteristics in TIG welding at pulsed change of current. When constructing such a model, the Kirchhoff equations, describing the electric circuit, were complemented by equations of the dynamic model of the arc as an element of the electric circuit [18]. Static VAC of the arc column and time constant of the transient process which is to be determined are used as parameters of the model with concentrated parameters. In order to identify these parameters, experimental studies of static VACs of an argon arc with a tungsten cathode and copper water-cooled anode were conducted. Time constant θ of the transient process was defined, proceeding from the calculated data on the dynamics of the change of arc voltage, derived using the model with distributed parameters [15].

The impact on the arc of trapezoidal current pulses with different front durations (20; 100; 200 μs) was considered. Calculations were conducted for a 3 mm argon arc with a refractory cathode. It was assumed that after current rise (drop) the arc burns at constant current until the steady state sets in. Results of calculation of dynamic VAC of such an arc for models with distributed and concentrated parameters are presented in Figure 17. The same Figure shows the respective values of θ, selected by the criterion of the best fit of the results of calculation using the above models.

As follows from the calculated data given in this Figure, the time constant decreases with reduction of the pulse front duration. A characteristic feature of the dynamic VAC of the arc is the fact that it is presented in the form of a hysteresis loop, in which the upper and lower curves correspond to the pulse leading and trailing edges, and the vertical sections — to transition into the arc stationary state. VAC of the arc in the form of a hysteresis loop was derived experimentally in works [19, 20]. The cause for its appearance is the different degree of inertia of the processes of transfer

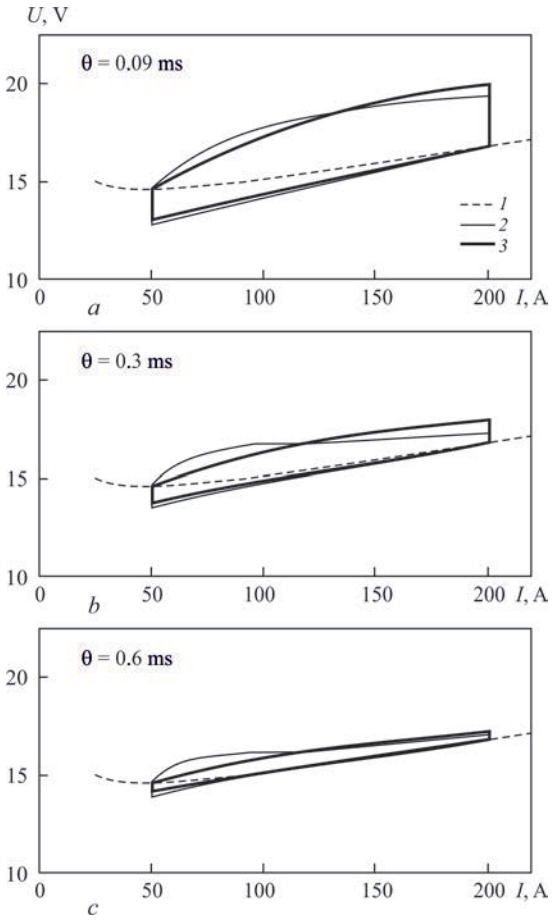

Figure 17. Dynamic VACs of the arc at the following duration of pulse fronts: 20 μs: (*a*) 100 μs (*b*) and 200 μs (*c*): *1* — static VAC of the arc; *2* — dynamic VAC of the arc (model with distributed parameters); *3* – dynamic VAC (model with concentrated parameters) [5]

of energy, pulse and charge at current rise and drop. Note that with increase of pulse front duration the range of the hysteresis loop decreases, and dynamic VAC of the arc becomes closer to that of a stationary arc (see Figure 17, *c*).

Study [12] provides brief analysis of the impact of the parameters of pulse modulation of welding current on the characteristics of dynamic action of an arc with refractory cathode on weld pool metal. It is shown that the larger the square of the acting (effective) value of current I_E, the greater is the force applied to the molten metal. Thus, in order to ensure the

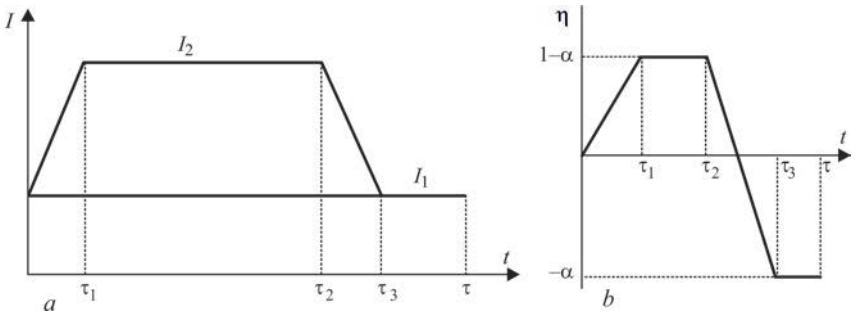

Figure 18. Schematic presentation of arc current pulse: *a* — trapezoidal pulse with a pause; *b* — respective normalized pulse (function) η(*t*) [21]

maximum above-mentioned action (at fixed average value of current I_A), the shape and time parameters of modulation pulses should be selected by the criterion of I_E maximum.

For any current $I(t)$ that periodically changes in time, the following representation is in place:

$$I(t) = I_A + A\eta(t), \qquad (19)$$

where $A = I_2 - I_1$ is the current modulation amplitude; I_1, I_2 are the minimum and maximum values of current; $\eta(t)$ is a certain normalized function, which contains information on the shape and time parameters of pulses. Considering a rather general case of welding current modulation by pulses of a trapezoidal shape, presented in Figure 18, the authors showed that

$$I_E^2 = I_A^2 + A^2 f(\xi, \gamma);$$
$$f(\xi,\gamma) = \xi\left[\frac{2}{3}(1+2\gamma) - \xi(1+\gamma)^2\right], \qquad (20)$$

where dimensionless parameters $\xi = \frac{\tau_3}{2\tau}\left(0 < \xi \le \frac{1}{2}\right)$ and $\gamma = \frac{\tau_2 - \tau_1}{\tau_3}(0 \le \gamma \le 1)$ characterize relative pulse duration (equal to half of the duty cycle) and its shape (at $\gamma = 0$ the trapezoidal pulse becomes triangular, and at $\gamma = 1$ — it is rectangular, respectively), and the average value of current can be written as $I_A = (1 - \alpha)I_1 + \alpha I_2$, where $\alpha = \frac{\tau_3 + \tau_2 - \tau_1}{2\tau}(0 \le \alpha \le 1)$.

Figure 19 shows the behaviour of function $f(\xi, \gamma)$, from the explicit form of which it follows that the effective value of modulated current depends on the duty cycle and shape of pulses and does not depend on the frequency of their flowing. Note also that $f(\xi, \gamma) \ge 0$, i.e. the square of effective value of current is always greater than the square of its average value.

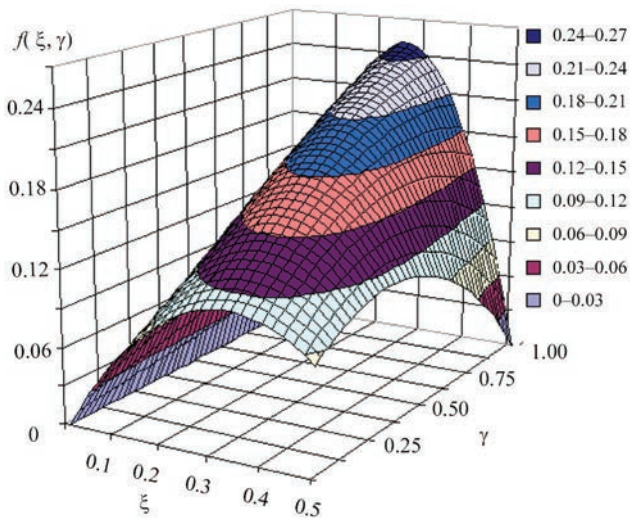

Figure 19. Appearance of function $f(\xi, \gamma)$ [21]

As follows from (20), in order to ensure maximum value of I_E at fixed values of I_A and A, the parameters should be chosen so that function $f(\xi, \gamma)$ took the greatest value. For trapezoidal pulses (see Figure 18) parameter α is equal to $\xi(1 + \gamma)$. Therefore, at analysis of function $f(\xi, \gamma)$ not the entire range of the change of parameters ξ, γ, but just their values satisfying equations $\alpha = \xi(1 + \gamma)$ should be considered. Expressing from this equation γ through ξ, α, we get $f(\xi, \alpha) = \frac{4}{3}\alpha - \alpha^2 - \frac{2}{3}\xi$. This function decreases monotonically with ξ increase and has the greatest value at minimum value ξ_{min}. In the case of triangular pulses ($\gamma = 0$) we find $\xi = \alpha$, and in the case of rectangular pulses ($\gamma = 0$), we have $\xi = \frac{\alpha}{2}$. Thus, minimum value of $\xi_{min} = \frac{\alpha}{2}$, that provides the greatest value of function $f(\xi_{min}, \alpha) = \alpha - \alpha^2$ at the set α, is achieved in the case, when $\gamma = 0$. Function $\alpha - \alpha^2$ has a maximum at $\alpha = 0.5$, that gives $\xi = 0.25$, i.e. this set of dimensionless parameters corresponds to rectangular pulses in the form of a meander.

As it is impossible to achieve a rectangular shape of current pulses in practice, in [21] the behaviour of function $f(\xi, \gamma)$ was studied for the case of a trapezoidal current pulse. Designating as $\tau_f = \tau_1 + \tau_3 - \tau_2$ the total duration of the pulse leading and trailing edges (see Figure 18, *a*), we can show that the minimum value of ξ is determined as follows: $\xi_{min} = \frac{\alpha}{2 - \bar{\tau}_f}$, where $\bar{\tau}_f = \frac{\tau_f}{\tau_3}$. Hence, $f(\xi_{min}, \alpha) = \frac{2}{3}\left(2 - \frac{1}{2 - \bar{\tau}_f}\right)\alpha - \alpha^2$. This function has a maximum, equal to $f(\bar{\tau}_f) = \frac{1}{9}\left(2 - \frac{1}{2 - \bar{\tau}_f}\right)^2$, at $\alpha = \frac{1}{3}\left(2 - \frac{1}{2 - \bar{\tau}_f}\right)$.

Analysis of the results of the works, devoted to modeling the processes of TIG welding by modulated current, leads to the following conclusions:

1. Results of theoretical analysis of the characteristics of an arc with a refractory cathode at high-frequency pulse modulation of current confirm the effects of arc constriction and increase of pressure of arc plasma flow on the anode surface, compared to that of a direct current arc that was observed experimentally. It is shown, for instance, that the pressure of an arc with HFP modulation of current rises with decrease of the duty cycle (at constant average value of arc power) in proportion to the ratio of squares of effective and average values of modulated current.

2. Mathematical models of thermal, hydrodynamic and electromagnetic processes in the metal being welded (also at self-consistent accounting for the processes proceeding in arc plasma) were developed, according to the conditions of spot TIG welding with low-frequency (f < 10 Hz) modulation of welding current. Detailed computer modeling of the above-mentioned processes was performed, the results of which are in good agreement with the experimental data.

3. The questions of modeling the distributed characteristics of plasma of a nonstationary arc with a refractory cathode and its action on the surface of the metal being welded, in TIG welding with HFP modulation of welding current (f > 10 kHz) is not given sufficient attention in modern scientific-technical publications (except for works [5, 14]). Therefore, it is believed to be rational to conduct detailed theoretical studies and mathematical modeling of the processes of energy-, mass- and electric transfer in the system of «nonstationary arc–metal being welded» at TIG welding with HFP modulation of current.

1. Boyi, Wu, Krivtsun, I.V. (2019) Processes of nonconsumable electrode welding with welding current modulation (Review). Part 1. Peculiarities of burning of nonstationary arcs with refractory cathode. *The Paton Welding J.*, **11**, 23–32.
2. Boyi, Wu, Krivtsun, I.V. (2019) Processes of nonconsumable electrode welding with welding current modulation (Review). Part 2. Effects of arc impact on the metal being welded. *The Paton Welding J.*, **12**, 11–23.
3. Yamaoto, T., Shimada, W., Gotoh, T. (1976) *Characteristics of high frequency pulsed DC TIG welding process.* Doc. IIW 212-628–76, 11–23.
4. Cook, G.E., Eassa, H.E.-D.E.H. (1985) The effect of high-frequency pulsing of a welding arc. *IEEE Transact. on Industrial Application*, 1A–21, **5**, 1294–1299.
5. Sydorets, V.N., Krivtsun, I.V., Demchenko, V.F. et al. (2016) Calculation and experimental research of static and dynamic volt-ampere characteristics of argon arc with refractory cathode. *The Paton Welding J.*, **2**, 2–8.
6. Kim, W.H., Na, S.J. (1998) Heat and fluid flow in pulsed current GTA weld pool. *Int. J. of Heat and Mass Transfer.*, 41(**21**), 3213–3227.
7. Lee, S.Y., Na, S.J. (1996) A numerical analysis of a stationary gas tungsten welding arc considering various electrode angle. *Weld. J., Res. Suppl.*, 269–279.
8. Kim, W.H., Fan, H.G., Na, S.J. (1997) A mathematical model of gas tungsten arc welding considering the cathode and the free surface. *Metall. Transact.*, **28B**, 679–686.
9. Wu, C.S., Zheng, W., Wu, L. (1999) Modelling the transient behaviour of pulsed current tungsten-inert-gas weld pools. *Modelling and Simul. Mater. Sci. Eng.*, 7(**1**), 15–23.
10. Wu, C.S. (2008) *Welding heat process and pool geometry*. Beijing, China Machine Press, 102–104.
11. Traidia, A., Roger, F., Guyot, E. (2010) Optimal parameters for pulsed gas tungsten arc welding in partially and fully penetrated weld pools. *Int. J. of Thermal Sci.*, **49**, 1197–1208.
12. Traidia, A., Roger, F. (2011) Numerical and experimental study of arc and weld pool behaviour for pulsed current GTA welding. *Int. J. of Heat and Mass Transfer*, **54**, 2163–2179.
13. Yang, M., Qi, B., Cong, B. et al. (2013) Study on electromagnetic force in arc plasma with UHFP-GTAW of Ti–6Al–4V. *IEEE Transact. on Plasma Sci.*, 41(**9**), 2561–2568.
14. Krivtsun, I.V., Krikent, I.V., Demchenko, V.F. (2013) Modelling of dynamic characteristics of a pulsed arc with refractory cathode. *The Paton Welding J.*, **7**, 13–23.
15. Krikent, I.V., Krivtsun, I.V., Demchenko, V.F. (2012) Modelling of processes of heat-, mass- and electric transfer in column and anode region of arc with refractory cathode. *Ibid*., **3**, 2–6.
16. Yang, M., Yang, Z., Cong, B. et al. (2014) A study on the surface depression of the molten pool with pulsed welding. *Welding J., Res. Suppl.*, 93(**8**), 312–319.
17. Yang, M., Yang, Z., Qi, B. (2015) The effect of pulsed frequency on the plasma jet force with ultra high frequency pulsed arc welding. *IIW*, **8**, 875–882.
18. Sydorets, V.N., Pentegov, I.V. (2013) *Deterministic chaos in nonlinear circuits with electric arc*. Kiev, IAW [in Russian].
19. Sokolov, O.I., Gladkov, E.A. (1977) Dynamic characteristics of free and constricted welding arcs of direct current with nonconsumable electrode. *Svarochn. Proizvodstvo*, **4**, 3–5 [in Russian].
20. Trofimov, N.M., Sinitsky, R.V. (1967) Dynamic characteristics of pulsed arc in argon arc welding. *Ibid*., **8**, 18–19 [in Russian].
21. Demchenko, V.F., Boi, U., Krivtsun, I.V., Shuba, I.V. (2017) Effective values of electrodynamic characteristics of the process of nonconsumable electrode welding with pulse modulation of arc current. *The Paton Welding J.*, **8**, 2–11.

Received 21.12.2019